Eur. Phys. J. B **62**, 123–128 (2008)
DOI: 10.1140/epjb/e2008-00146-5

THE EUROPEAN PHYSICAL JOURNAL B

Magnetization and specific heat of $DyFe_3(BO_3)_4$ single crystal

E.A. Popova[1,a], N. Tristan[2], A.N. Vasiliev[1], V.L. Temerov[3], L.N. Bezmaternykh[3], N. Leps[2], B. Büchner[2], and R. Klingeler[2]

[1] Low Temperature Physics Department, Moscow State University, 119991 Moscow, Russia
[2] Leibniz Institute for Solid State and Materials Research, IFW Dresden, 01171 Dresden, Germany
[3] L.V. Kirensky Institute of Physics, Siberian Branch of RAS, Krasnoyarsk, 660036, Russia

Received 12 November 2007 / Received in final form 18 February 2008
Published online 11 April 2008 –

Abstract. We present thermodynamic and magnetic studies of single crystalline $DyFe_3(BO_3)_4$. The data indicate an easy axis antiferromagnetic order below $T_N \sim 38$ K which we attribute to the Fe subsystem. The Dy subsystem remains paramagnetic down to the lowest investigated temperatures of 2 K, but it is polarized by the Fe spins due to a $f-d$ interaction. External magnetic field leads to a spin-flop transition in the iron subsystem as well as to superposed magnetization in the Dy subsystem. The repopulation of two low-lying Kramers doublets in Dy^{3+} ions results in well defined Schottky anomalies in specific heat and magnetization.

PACS. 75.30.-m Intrinsic properties of magnetically ordered materials – 75.40.Cx Static properties

1 Introduction

The rare-earth ferroborates with the general formula $RFe_3(BO_3)_4$ (R is yttrium or a rare-earth ion) constitute a large family of metal-oxide compounds. Their study reveals important features of $3d$- and $4f$-electrons interactions. Besides purely magnetic effects, the interplay of electric and magnetic order parameters is of interest, because it has already been shown that some members of this family possess multiferroic properties [1–3]. At high temperatures, the $RFe_3(BO_3)_4$ compounds belong to the trigonal space group D_3^7 (R32). In this structure, chains of edge-sharing FeO_6 octahedra run along the trigonal axis, being interconnected by isolated RO_6 trigonal prisms and BO_3 triangles [4]. Within this family, the members with $R = Eu - Er$ experience a first order structural transformation to a less symmetric $P3_121$ phase which also belongs to the trigonal type [5].

At low temperatures, every compound of this family exhibits an antiferromagnetic order at the Néel temperature T_N which only slightly depends on the kind of rare-earth ions [5]. To that same range falls the T_N in $YFe_3(BO_3)_4$, indicating that the rare-earth does not influence much the ordering in the iron subsystem. Whereas, the particular type of magnetic structure, i.e. either easy-axis or easy-plane order, depends on the anisotropy of the R^{3+} ion. Thus, it was found that at $T_N = 37$ K, the $GdFe_3(BO_3)_4$ compound orders antiferromagnetically into the collinear easy-plane structure, at $T_R = 10$ K, a reorientation of the magnetic moments to the easy-axis magnetic structure occurs [6–9]. In $NdFe_3(BO_3)_4$, the magnetic moments of both iron and neodymium ions are oriented in the ab-plane [10,11], while in $TbFe_3(BO_3)_4$, the magnetic moments of both iron and terbium subsystems are aligned with the trigonal c-axis [12].

The application of external magnetic field to rare-earth ferroborates results in field induced transitions. The reorientation of magnetic moments caused by a magnetic field also leads to noticeable changes in dielectric permittivity and polarization. It was found, that the magnetoelectric effects are much stronger in $NdFe_3(BO_3)_4$ than in the isostructural $GdFe_3(BO_3)_4$ compound [1,2,13].

In the present paper, we report magnetization and specific heat studies of $DyFe_3(BO_3)_4$ single crystal. The magnetic measurements show that, below T_N, the magnetic moments of the iron and dysprosium subsystems are aligned along the trigonal axis, which is in agreement with theoretical predictions [14] and optical investigations [15]. Such orientation of magnetic moments causes a spin-flop transition in the iron subsystem in a magnetic field applied along the trigonal axis, while the magnetic moment of dysprosium subsystem aligns in the direction of the external magnetic field. At low temperatures, the repopulation of two low-lying Kramers doublets in Dy^{3+} ions results in well defined Schottky anomalies in specific heat and magnetic susceptibility.

[a] e-mail: eapopova@yahoo.com

2 Experimental

Single crystals of $DyFe_3(BO_3)_4$ were grown using a $Bi_2Mo_3O_{12}$-based flux [16]. Seeds were obtained by spontaneous nucleation from the same flux. Single crystals are green in colour and have good optical quality and easily visible grown edges. Magnetic susceptibility $\chi(T)$ measurements were performed in the temperature range of 2–350 K in a magnetic field of $B = 0.05$ T using a commercial Quantum Design SQUID magnetometer. Magnetization measurements were performed in a home built vibrating sample magnetometer [17] in magnetic fields up to 15 T while sweeping the field at a rate of 0.4 T/min and, at 4.2 K, in pulsed magnetic fields up to 48 T with pulse duration of approximately 0.05 s. All magnetic measurements were carried out in magnetic fields oriented along the crystallographic a, c and b'-axes. The last direction is not a crystallographic axis of the trigonal crystal, but it points perpendicularly to the crystallographic a- and c-axes. Heat capacity was measured in the temperature range of 2–300 K using a Quantum Design Physical Properties Measurement System.

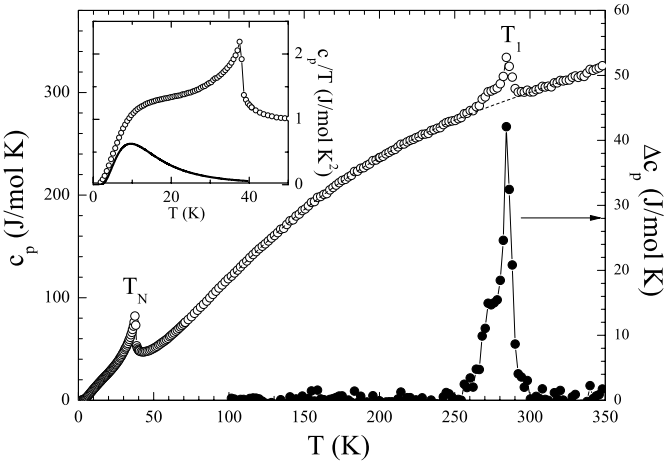

Fig. 1. The temperature dependence of specific heat (open circles) and the excessive specific heat (closed circles) estimated by subtracting continuous background (dashed line) from total specific heat. Inset: c_p/T vs. T dependence (open circles) and Schottky anomaly (solid line) calculated according to the model discussed in the text.

3 Results

The measurements of the specific heat c_p in zero magnetic field and of the magnetic susceptibility χ along different crystal directions in a small field of $B = 0.05$ T (see Figs. 1 and 2) display the basic properties of $DyFe_3(BO_3)_4$. The specific heat data exhibit several pronounced anomalies, i.e. a first order phase transition at $T_1 \sim 280$ K, a second order transition indicated by a λ-type anomaly at about 38 K, and a Schottky-type anomaly around 10 K. Overall, the magnetic susceptibility exhibits a Curie-Weiss-like temperature dependence above 38 K and a decrease of the magnetization upon further cooling. The anomalies of c_p are associated with only small changes in magnetizsation. In particular, the data in Figure 2 barely show any feature at 280 K, and at 38 K there is a kink only in $\chi \| c$. Upon further cooling, the data display broad maxima in $B \| c$ and $B \| a, b'$ at 23 K and 10 K, respectively. In addition, we find a slight upturn at very low temperatures which we attribute to the presence of a small amount of paramagnetic impurities.

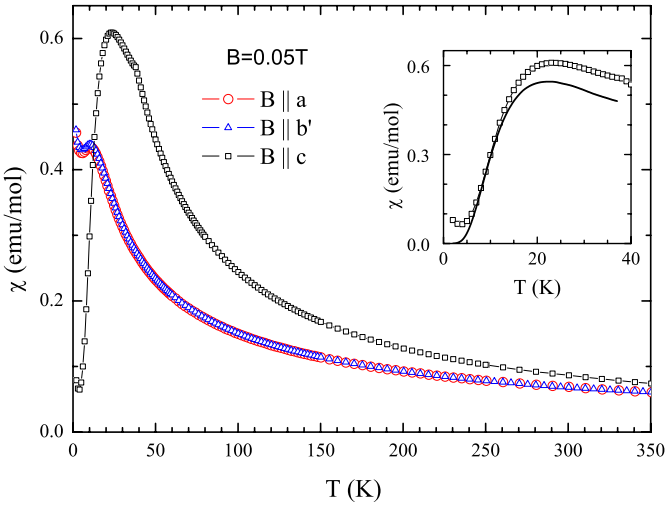

Fig. 2. The temperature dependence of magnetic susceptibility $\chi = M/H$ measured in $B = 0.05$ T along a, b' and c axes. Inset: $\chi_c(T)$ dependence enlarged in the low temperature range (symbols) and Schottky-type anomaly (solid line) calculated according to the model discussed in the text.

We presume that the high temperature specific heat anomaly seen at about 280 K is related to a structural transformation. This notion is supported by the observation that a structural transformation is observed in a powder sample of $DyFe_3(BO_3)_4$ at 340 K [5]. The difference between the transition temperature T_1 in the single crystal studied here and in the ceramic sample might indicate a high sensitivity of the chemical composition of dysprosium ferroborate to the method of preparation. The single crystals grown in $Bi_2Mo_3O_{12}$-based flux could adsorb Bi^{3+} ions which can partially substitute Dy^{3+} ions in the structure. Indeed, small traces of Bi were found in our single crystals by EDX analysis. In addition, the specific heat data display a shoulder below T_1 which might be associated to a structural non-uniformity of the sample. Nevertheless, the comparison of the magnetic transition temperature of the single crystal with that of the ceramic sample [5] implies that a slight dilution of the rare-earth subsystem does not change the magnetic parameters of the transition metal subsystem. This conclusion is consistent with the absence of a similar feature as the shoulder below T_1 in the proximity of the magnetic ordering transition at T_N. If one assumes a continuous background of the specific heat as it is indicated by the dashed line in Figure 1, the data imply that the anomalous entropy change at T_1 amounts to $\int \Delta c_p/T \, dT \approx 1.9$ J/molK.

The high temperature magnetic properties exhibit considerable magnetic anisotropy. While $\chi_a(T)$ and $\chi_{b'}(T)$ practically coincide across the entire temperature range, $\chi_c(T)$ is considerably larger than $\chi_a(T)$ and $\chi_{b'}(T)$. Since no significant magnetic anisotropy is expected for the 3d-ion Fe^{3+}, we attribute the high temperature anisotropy to the Dy^{3+} subsystem. We note that the data can not be described in terms of the Curie-Weiss law. For temperatures higher than the crystal field splitting, one would expect uniform population of the levels and an isotropic Curie-Weiss-like magnetization. The data hence imply that the splitting of the energy levels is at least larger than ∼400 K.

The λ-type anomaly found in the specific heat at 38 K as well as the kink in the magnetic susceptibility $\chi_c(T)$ indicate the onset of long range magnetic order. This temperature agrees to the Néel temperature found in a polycrystalline sample of $DyFe_3(BO_3)_4$ [5] and by means of spectroscopy measurements on a single crystal [15]. The magnetic susceptibility data in Figure 2 indicate complex temperature dependence in the spin ordered phase. The low temperature behaviour of the in-plane and out-of-plane magnetic susceptibilities and the fact that $\chi_c(T)$ tends to vanish approaching zero temperature suggests that at 38 K, the system undergoes an antiferromagnetic transition so that the magnetic moments of both the rare-earth and transition metal subsystems are oriented along the trigonal c-axis. However, the contribution of the rare earth subsystem to the total magnetic susceptibility of $DyFe_3(BO_3)_4$ complicates the behaviour so that the magnetic susceptibility does not correspond to a typical easy-axis antiferromagnet. Instead, we observe broad maxima at about 11 K in $\chi_c(T)$ and at about 23 K in $\chi_a(T)$ and $\chi_{b'}(T)$. We attribute these maxima and the broad anomaly in the specific heat at $T < T_N$ to the thermal population of two low-lying Kramers doublets of the Dy^{3+} ions, i.e., a Schottky anomaly (a detailed analysis will be given below).

The magnetization dependences $M_a(B)$ and $M_c(B)$ measured at $T = 4.2$ K along the a- and c-axes and a derivative dM_c/dB are shown in Figure 3. In low fields, $M_c(B)$ increases gradually, and it shows a negative curvature at least above 1.5 T. At the critical field $Bcr \sim 3$ T, the magnetization exhibits a sharp jump reaching a value of $\sim 7\mu_B$ immediately after the transition. A further increase of the magnetic field leads to a subsequent linear increase of the magnetization. A small hysteresis at the critical field B_{cr} points to a first order character of the phase transition. In a pulsed field (see Fig. 4) the hysteresis of the magnetization $M_c(B)$ is noticeably larger than in a static field (Fig. 3). This can be caused either by relaxation processes related to the first order transition or by the magnetocaloric effect. In contrast, the magnetization along the a-axis $M_a(B)$ increases gradually, has positive curvature below 20 T, and does not exhibit any sharp anomalies. It is worth mentioning that above ∼20 T the magnetization measured along both axes is anisotropic but increases linearly with an isotropic slope of $\chi \sim 8 \times 10^{-2}$ erg/(G^{2}mol) up to 48 T.

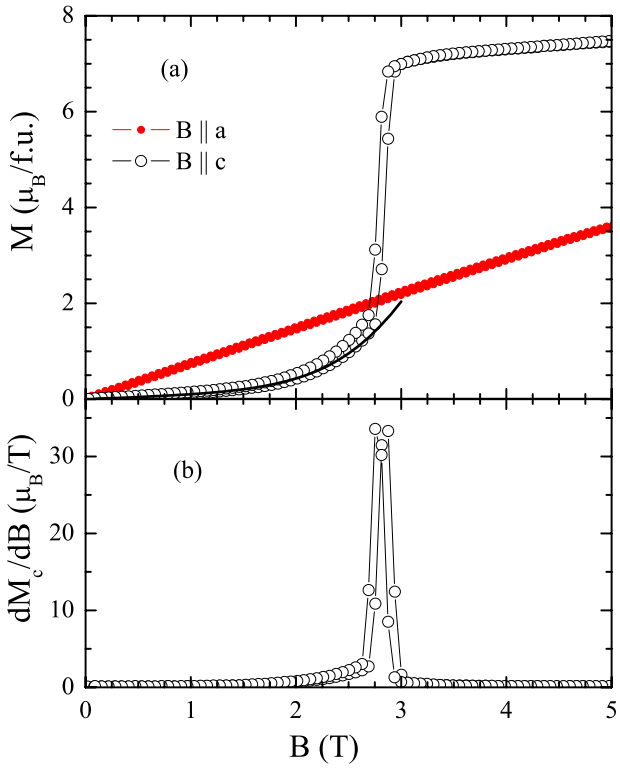

Fig. 3. (a) The magnetic field dependences $M(B)$ measured along a (filled circles) and c (open circles) axes at 4.2 K in static magnetic field. Solid line represents fitted curve (see text for details). (b) The peaks on the dependences of dM/dB vs. B indicate critical fields of the first order phase transition.

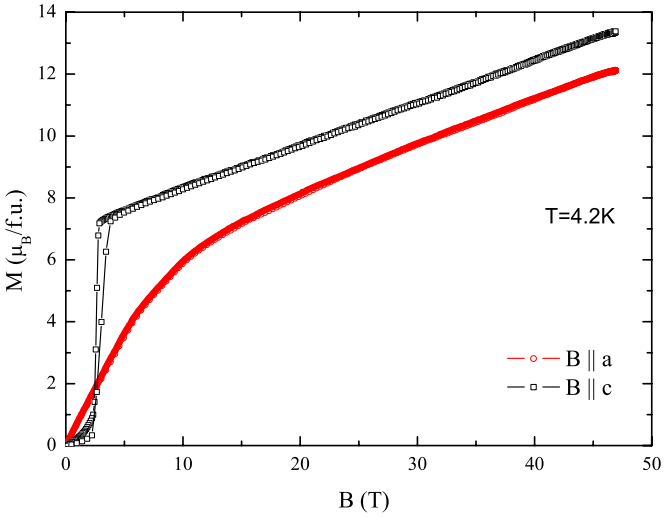

Fig. 4. The magnetic field dependences M(B) measured along a (filled circles) and c (open circles) axes at 4.2 K in pulsed magnetic field.

The magnetization dependences $M_a(B)$ and $M_c(B)$ investigated at different temperatures in magnetic fields up to 15 T are shown in Figure 5. At higher temperatures, the magnetization jump in $M_c(B)$ decreases in value and shifts to the higher fields. Above T_N, no jump-like anomalies were observed in the $M_c(B)$ dependences. No such anomalies were found in the $M_a(B)$ dependences at any

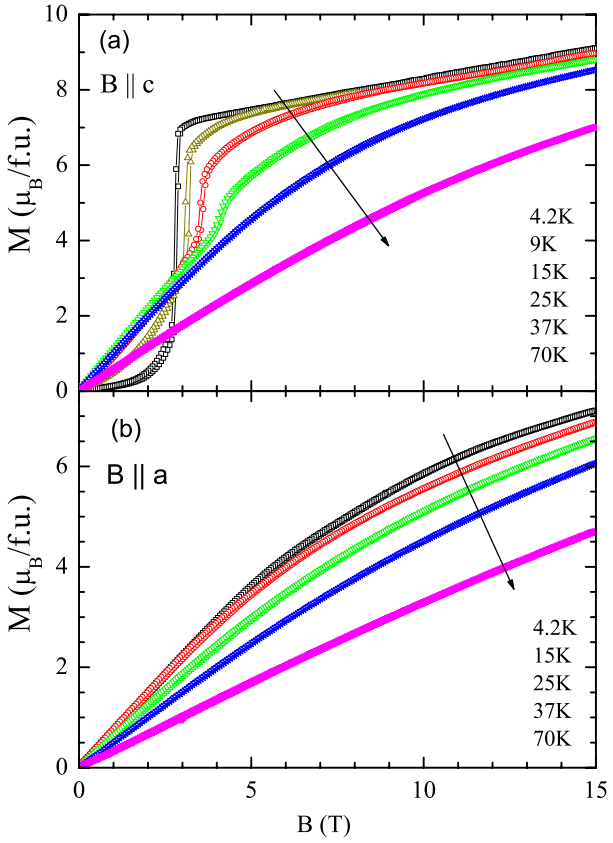

Fig. 5. The magnetization curves measured in static magnetic field at different temperatures along (a) c and, (b) a axes.

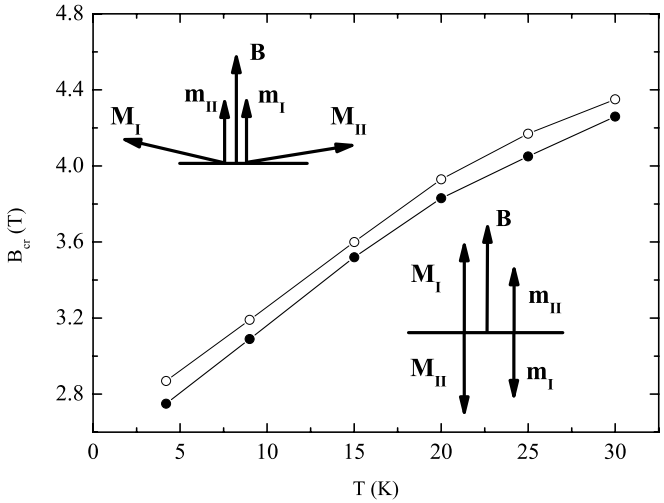

Fig. 6. Magnetic phase diagram for $B\|c$ obtained from magnetization data. B_{cr} labels the critical field of the spin-flop transition. Full/open data markers refer to increasing/decreasing quasi-static fields, i.e., $\partial B/\partial t \sim 0.4$ T/min (see text). M is the magnetic moment of iron ion, m is the magnetic moment of dysprosium ion, I and II are numbers of sublattices.

temperature, and in the temperature range $T < T_N$ they always had a positive curvature. The observed anomalies are summarized in the phase diagram in Figure 6.

4 Discussion

The magnetic system of $DyFe_3(BO_3)_4$ consists of two kinds of magnetic ions, i.e., Fe^{3+} and Dy^{3+}, which contribute to its magnetic properties. Our experimental data can be understood if one assumes that the magnetic ordering takes place in the iron subsystem only while the dysprosium subsystem remains essentially paramagnetic. In this model, the dysprosium subsystem is polarized due to $f-d$ interaction and can be considered as two sublattices with the magnetic moments oriented along the trigonal axis in zero external magnetic field. In contrast to the two sublattices of the iron subsystem which are coupled by an antiferromagnetic exchange interaction, the sublattices of the dysprosium subsystem do not strongly interact with each other.

As mentioned above, at low temperature, the magnetic moments of both the rare-earth and the iron subsystem are aligned along the c-axis. The magnetic field driven jump in $M_c(B)$ corresponds to a spin–flop transition in the iron subsystem, i.e., the magnetic moments of the Fe^{3+}–ions flop into the plane perpendicular to the c-axis. The small hysteresis observed on $M(B)$ dependences indicates that the spin-flop transition in the iron subsystem is of the first order. The spectroscopic data [18] show that the crystal field acting on dysprosium ions leads to splitting between the first and second Kramers doublets of about 15.5 cm^{-1}, and between the first and third doublets of about 140 cm^{-1}. This crystal field splitting causes a strong anisotropy of the Dy ion. Thus, immediately after the spin-flop transition, the magnetic moments of both dysprosium sublattices align along the direction of an external magnetic field. This results in a jump of overall magnetization. The shift of the critical field of this transition to higher values and the reduction of the magnetization jump with increasing temperature relates to the diminishing difference between $\chi_{\perp}^{Fe}$ and $\chi_{\parallel}^{Fe}$.

At $T = 4.2$ K in the external field $B\|c < B_{cr}$, the magnetic susceptibility of the iron subsystem $\chi_{\parallel}^{Fe}$ is very small. The shape of $M_c(B)$ dependence in fields $B < B_{cr}$ is predominantly determined by the behaviour of the dysprosium subsystem. The effective field B_{eff} acting on the dysprosium sublattice with the magnetic moment directed opposite to the external field decreases, and, therefore, this magnetic moment tends to diminish with increasing field. At the same time, the effective field favours an increase of the magnetization of the dysprosium sublattice with magnetic moments aligned with the external field. This leads to a gradual increase in the total magnetic moment and implies the concave character of the magnetization at low fields.

In order to estimate the contribution of the dysprosium subsystem to the magnetization and the specific heat below the Néel temperature, we have to take the splitting

of the Dy^{3+} energy levels (total momentum $J = 15/2$) into account. Any crystal field with symmetry lower than a cubic one results in eight Kramers doublets. The spectroscopic data show that, at zero field, the splitting between the first and second Kramers doublets amounts to $\Delta = 15.5\ \mathrm{cm}^{-1} = 22.3$ K, and the population of the others is negligibly small for $T < T_N$ [15]. Hence, below the Néel temperature, only these two lowest doublets contribute to the magnetic properties. The external magnetic field results in a further splitting of the Kramers doublets. The magnetic moment per dysprosium ion can be written as

$$M_\alpha = \frac{\mu_B}{2} \cdot \frac{g_1(e^{x_1} - e^{-x_1}) + g_2\, e^{-\Delta/kT}(e^{x_2} - e^{-x_2})}{(e^{x_1} + e^{-x_1}) + e^{-\Delta/kT}(e^{x_2} - e^{-x_2})}, \quad (1)$$

where α represents dysprosium sublattices with the magnetic moments oriented along ($\alpha = I$) or opposite ($\alpha = II$) to the direction of the external field, k is the Boltzmann constant, μ_B is the Bohr magneton, g_i ($i = 1$ or 2) are the components of g – tensor for the ground and the second Kramers doublets, respectively, and the variable $X_i = \frac{g_i \mu_B B_{eff}}{2kT}$. Here, the effective magnetic field acting on the Dy^{3+} ions, B_{eff}, results from both the external field B and the internal field, B_{f-d}, from the ordered Fe subsystem. In the case of the I_{st} dysprosium sublattice, the effective magnetic field is $B_{eff} = B + B_{f-d}$, and in the case of the IInd sublattice, it is $B_{eff} = B - B_{f-d}$. At $T = 4.2$ K and for $B \| c < B_{cr}$, $M_c(B)$ can be described as a superposition of two contributions, $M = 0.5(M_I + M_{II})$, where each contribution corresponds to one of the two dysprosium sublattices with appropriate B_{eff}.

We assume, that the value of magnetization, reached immediately after the spin-flop transition, $M_{sf} = 6.8\ \mu_B$, corresponds to the phase where the magnetic moments of both dysprosium sublattices are oriented along the external magnetic field and the iron spins are oriented perpendicular to the field. This value as well as value of $\Delta = 15.5\ \mathrm{cm}^{-1}$ allows one to fit the low field magnetization along the c axis using equation (1). The results of fitting are shown in Figure 3a by the solid line. This procedure yields the g-factors of the two low-lying doublets and the exchange interaction between the transition and the rare earth sublattice. We find that $g_1 = 13.1$, $g_2 = 16$ and $B_{f-d} = 3.4$ T, respectively. We note that, in order to achieve the best fitting results, an additional linear term was added which probably arises due to thermal fluctuations in the iron subsystem above zero temperature. We also can not exclude a small amount of paramagnetic impurities.

The parameters, g_1, g_2 and B_{f-d}, were used to estimate the contribution of the Dy^{3+} subsystem to magnetic susceptibility, $\chi_c^{Dy}(T)$, and specific heat, $c_{Schottky}(T)$. $\chi_c^{Dy}(T)$ was calculated by differentiating $M_c(T)$ from the equation (1) with respect to the magnetic field, and $c_{Schottky}(T)$ was calculated using standard formulas adjusted to the magnetic structure model described above taking into account the temperature dependence of the internal magnetic field, B_{f-d} [15]. The results, shown in the insets of Figures 1 and 2, provide additional support for the suggestion that the broad maximum in $\chi_c(T)$ at ~23 K and the wide anomaly below T_N in the specific heat can be associated with the repopulation of two low-lying Kramers doublets of Dy^{3+} ions.

In the flop phase ($B > B_{cr}$), the magnetic moments of the iron subsystem continuously rotate towards the applied magnetic field. The linear slope of $M_c(B)$ is governed by the Fe^{3+}-spins, i.e., $M_\perp^{Fe} = \chi_\perp^{Fe} B$, so that the perpendicular susceptibility of the iron subsystem can be estimated as $\chi_\perp^{Fe} \approx 0.14 \mu_B / T$.

To understand further details of the experimental data and to perform a reliable analysis of the field and temperature dependence of the in-plane magnetic response, the strict calculation of the energy level splitting caused by the crystal and external magnetic fields must be carried out. However, we can postulate that the wide maximum of the in-plane magnetic susceptibility around 11 K is again related to the repopulation of the two low-lying Kramers doublets in Dy^{3+} ions, as is the case for $\chi_c(T)$ at ~23 K. The lower temperature of the Schottky anomaly can be caused by smaller values of the in-plane g-factors in comparison to those out-of-plane.

If the magnetic field is oriented within the basal plane, the magnetic moments of both the rare-earth and iron subsystems rotate towards the field direction as the field increases. The total magnetization can be estimated as $M_a(B) = \chi_\perp^{Fe} B + M_{Dy}$, where $\chi_\perp^{Fe} B$ and M_{Dy} are the contribution of the iron and the dysprosium subsystems, respectively. Since above 20 T the slope of $M_a(B)$ is the same as the slope of $M_c(B)$, we can assume that in high fields, the increase of the total magnetization $M(B)$ is caused only by the iron subsystem. The magnetic moment of the dysprosium subsystem reaches ~5 μ_B at about 20 T and remains unchanged up to the maximum investigated field.

5 Conclusion

The experimental data on the thermodynamic properties of $DyFe_3(BO_3)_4$ clearly show that below $T_N = 38$ K, the compound is an easy-axis antiferromagnet. However, the magnetic susceptibility and magnetization data indicate that the magnetic contributions of the rare-earth and transition metal subsystems differ qualitatively. The iron subsystem orders antiferromagnetically below T_N, while the dysprosium subsystem remains essentially paramagnetic down to the lowest investigated temperatures. The paramagnetic behaviour of the dysprosium subsystem, polarized due to $f-d$ interaction, is additionally complicated by the splitting of the two lowest Kramers doublets of the Dy^{3+} ions. The broad maximum in the magnetic susceptibility $\chi_c(T)$ at ~23 K as well as an anomaly in specific heat $c_p(T)$ below T_N can be explained by the repopulation of the two lowest Dy^{3+}-energy levels.

This work was supported by RFBR grants 06-02-16088 and 07-02-92000, ISTC grant 3501, DFG grant 486 RUS 113. Support by the Deutsche Forschungsgemeinschaft through HE-3439/6 is gratefully acknowledged.

References

1. A.K. Zvezdin, S.S. Krotov, A.M. Kadomtseva, G.P. Vorob'ev, Yu.F. Popov, A.P. Pyatakov, L.N. Bezmaternykh, E.A. Popova, JETP Lett. **81**, 272 (2005)
2. A.K. Zvezdin, G.P. Vorob'ev, A.M. Kadomtseva, Yu.F. Popov, A.P. Pyatakov, L.N. Bezmaternykh, A.V. Kuvardin E.A. Popova, JETP Lett. **83**, 509 (2006)
3. F. Yen, B. Lorenz, Y.Y. Sun, C.W. Chu, L.N. Bezmaternykh, A.N. Vasiliev, Phys. Rev. B **73**, 054435 (2006)
4. J.A. Campá, C. Cascales, E. Gutierrez-Puebla et al., Chem. Mater. **9**, 237 (1997)
5. Y. Hinatsu, Y. Doi, K. Ito, M. Wakeshima, A. Alemi, J. Solid State Chem. **172**, 438 (2003)
6. A.D. Balaev, L.N. Bezmaternykh, I.A. Gudim, V.L. Temerov, S.G. Ovchinnikov, S.A. Kharlamova, J. Magn. Magn. Mat. **259**, 532 (2003)
7. A.I. Pankrats, G.A. Petrakovskii, L.N. Bezmaternykh, O.A. Bayukov, JETP **99**, 766 (2004)
8. R.Z. Levitin, E.A. Popova, R.M. Chtsherbov, A.N. Vasiliev, M.N. Popova, E.P. Chukalina, S.A. Klimin, P.H.M. van Loosdrecht, D. Fausti, L.N. Bezmaternykh, JETP Lett. **79**, 531 (2004)
9. S.A. Kharlamova, S.G. Ovchinnikov, A.D. Balaev, M.F. Thomas, I.S. Lyubutin, A.G. Gavriliuk, JETP. **101**, 1098 (2005)
10. E.A. Popova, N. Tristan, Ch. Hess, R. Klingeler, B. Büchner, L.N. Bezmaternykh, V.L. Temerov, A.N. Vasiliev, JETP **105**, 105 (2007)
11. D.V. Volkov, A.A. Demidov, N.P. Kolmakova, JETP **104**, 897 (2007)
12. E.A. Popova, D.V. Volkov, A.N. Vasiliev, A.A. Demidov, N.P. Kolmakova, I.A. Gudim, L.N. Bezmaternykh, N. Tristan, Yu. Skourski, B. Büchner, C. Hess, R. Klingeler. Phys. Rev. B **75**, 224413 (2007)
13. N. Tristan, R. Klingeler, C. Hess, B. Buechner, E. Popova, I.A. Gudim, L.N. Bezmaternykh, J. Magn. Magn. Mat. **316**, e621 (2007)
14. A.A. Demidov, N.P. Kolmakova, E.A. Popova, A.N. Vasiliev, D.V. Volkov, in Abstracts of Moscow Intern. Symp. on Magnetism (Moscow MSU, Moscow, Russia 2005), p. 668
15. T.N. Stanislavchuk, E.P. Chukalina, M.N. Popova, L.N. Bezmaternykh, I.A. Gudim, Phys. Lett. A **368**, 408 (2007)
16. L.N. Bezmaternykh, V.L. Temerov, I.A. Gudim, N.L. Stolbovaya, J. Crystallography Rep. **50** Suppl. 1, 97 (2005)
17. R. Klingeler, B. Büchner, K.-Y. Choi, V. Kataev, U. Ammerahl, A. Revcolevschi, J. Schnack, Phys. Rev. B **73**, 14426 (2006)
18. M.N. Popova, E.P. Chukalina, private communication